

SANDIA REPORT

RS-8232-2/069750

SAND89-8675
Unlimited Release
Printed November 1989



8232-2/069750

C.2



0000002 -

Spin a Tsuji-Burner and Create a Steady, Wrinkled, Strained Diffusion Flame?

To Appear in Combustion Science and Technology

Wm. T. Ashurst



Prepared by
Sandia National Laboratories
Albuquerque, New Mexico 87185 and Livermore, California 94551
for the United States Department of Energy
under Contract DE-AC04-76DP00789



Issued by Sandia National Laboratories, operated for the United States Department of Energy by Sandia Corporation.

NOTICE: This report was prepared as an account of work sponsored by an agency of the United States Government. Neither the United States Government nor any agency thereof, nor any of their employees, nor any of the contractors, subcontractors, or their employees, makes any warranty, express or implied, or assumes any legal liability or responsibility for the accuracy, completeness, or usefulness of any information, apparatus, product, or process disclosed, or represents that its use would not infringe privately owned rights. Reference herein to any specific commercial product, process, or service by trade name, trademark, manufacturer, or otherwise, does not necessarily constitute or imply its endorsement, recommendation, or favoring by the United States Government, any agency thereof or any of their contractors or subcontractors. The views and opinions expressed herein do not necessarily state or reflect those of the United States Government, any agency thereof or any of their contractors or subcontractors.

SAND89-8675
Unlimited Release
Printed November 1989

Spin a Tsuji-Burner and Create a Steady, Wrinkled, Strained Diffusion Flame?

Wm. T. Ashurst
Combustion Research Facility
Sandia National Laboratories
Livermore, CA 94551-0969

Abstract

Computed vorticity-flame interactions in two dimensions suggest that a wrinkled flame is a common occurrence in reacting turbulent flow and that these wrinkles are formed in a small fraction of an eddy turn-over time. An experiment in which the Tsuji porous-cylinder burner is spinning *may* be a way to achieve a steady, wrinkled diffusion flame under laboratory conditions. The wrinkled flame differs from the previously studied stagnation, counterflow flame in that the former has a large spatial variation in diffusive gradients near the wrinkle. These gradient variations may explain the extinction observed in unsteady, pulsed jets by Lewis *et al.*

A Tsuji-burner has been a popular experimental/computational device to simulate strained diffusion flames with the intent to obtain information that is appropriate for turbulent combustion. Fuel pumped through the porous cylinder reacts with the approach air flow. Near the stagnation streamline the flow field is characterized by the strain rate, and there are no diffusive fluxes along the flame surface. Thus, one-dimensional detailed and reduced kinetic calculations have been done (*cf.* Peters and Kee, 1987).

An aspect of turbulent flow which is not simulated is a wrinkled flame. Wrinkling is a ubiquitous feature of an interface in turbulent flow and the cause can be illustrated by convection of a non-diffusive scalar in a swirling flow. Consider two point vortices, separated a distance L in the y direction – a configuration typical of vortex structures in mixing layers. Start with scalar isolines parallel to the line joining the vortices, but offset from their x location. The offset is used to mimic flow past a splitter plate which generates a scalar interface between two vortical layers. In Figure 1, we show the scalar isolines after a small time period from these initial conditions, small with respect to the vortex turn-over time, $t_w = l/v = (2\pi r)^2/\Gamma$. We see that a wrinkle quickly forms and that the scalar gradient is larger on one side of the wrinkle (isolines closer together means larger scalar gradient). The isolines which are adjacent to the wrinkle and nearest to the vortex center have the highest gradient. Diffusive calculations indicate that the amount of wrinkling, or rotation around the vortex, is dependent on the Péclet number (Ashurst, 1989). Simulations with the flame-sheet model imply that the wrinkle is a local temperature maximum because the mixture fraction gradient is minimum at the wrinkle. This minimum is a result of the compressive strain-rate being parallel to the flame rather than normal, as in the counterflow case. Away from the wrinkle, the orientation of strain rate changes to being nearly normal, and so the scalar gradient is larger.

Examination of OH measurements of an unsteady diffusion flame near a vortex ring suggests, perhaps, that the wrinkle is burning hotter, while the flame near the vortex core has extinguished, and the other section of flame is still reacting (Figure 3c and 3d in Lewis *et al.*, 1988). These features would correspond to the gradient minimum, maximum and in-between value, see Figure 1. However, one needs to be cautious in the interpretation of OH measurements because the change in OH concentration with strain rate is small, only a one-third decrease as the strain rate is increased from near zero to near the extinction limit for methane (Chen, 1989).

So, it is suggested that a steady flow with a wrinkled flame can be created if the Tsuji-burner is spinning at a rate which moves the stagnation point from the front to the side of the cylinder. Based on potential flow, a circulation greater than $4\pi U_o R_c$ is sufficient,

which corresponds to 955 RPM when the cylinder radius R_c is 3 cm, as in the work of Tsuji and Yamaoka (1971), and the freestream velocity U_o is 150 cm/sec. (The zero-spin stagnation strain-rate is $2U_o/R_c$ and the critical spin-rate is $(2U_o/R_c)/(2\pi)$ in revolutions per time units, *cf.* Batchelor, 1967.) Potential streamlines are shown in Figure 2 for the value of $\Gamma/(4\pi U_o R_c) = 1.05$, which creates a small recirculation region on one side of the cylinder. The fuel flow rate is so small that its effect can not be seen in Figure 2, and so is not included.

We assume a constant-density flame and solve for the convection and diffusion of the mixture fraction Z in this steady potential-flow, but now include the fuel velocity, $V_{wall} = 0.05 U_o$. The Péclet number is 400 ($= U_o R_c / \alpha$, where α is the diffusivity). Mixture fraction isolines are shown in Figure 3 and contour values of $0.2 > Z > 0.02$ are of interest for hydrocarbon combustion; the pure fuel value of Z is unity. We see that the gradient of Z is almost constant on the front side of the recirculation region, and it is on the back side of the recirculation region where a curved "flame" may exist. Increasing the rotation rate reduces the scalar gradient in the curved region; $\Gamma/(4\pi U_o R_c) = 1.05$ and 1.2 are shown in Figures 3a and 3b.

It may be possible to set the strain rate so that the flame is quenched on the front or bottom-front of the cylinder, and thus only the curved flame would exist. This may require a continuous ignition source located somewhere in the flow, for example in some out-of-plane location. There also could be an optimum approach flow angle with respect to gravity so that buoyancy effects would be minimum (or heat the approach air flow). Close confinement with walls which are shaped like the potential streamlines (Fig. 2) may suppress boundary layer separation.

Another interesting configuration would be two spinning burners, with opposite rotation, arranged so that the recirculation regions are almost merged. Dilution of fuel in one burner may give a flame strip with a gradient of fuel/oxidizer boundary conditions. This would represent partial premixing that occurs in recting flows that have some quenching, that is a flame sheet with holes which allow mixing without reaction.

Thus, it may be possible to measure these steady-state flows and reaction profiles in curved flames. How these extra parameters are to be incorporated into reacting turbulence models is an area for future work.

Acknowledgement

This work was supported by the United States Department of Energy, through the Office of Basic Energy Sciences, Division of Chemical Sciences.

References

- Ashurst, Wm. T. (1989). Vorticity Generation in a Nonpremixed Flame Sheet. To appear in *Numerical Combustion* (A. Dervieux and B. Larrouturou, Eds., Lecture Notes in Physics, Springer-Verlag); also as Sandia Report SAND89-8592, June 1989.
- Batchelor, G. K. *An Introduction to Fluid Dynamics*, p. 427, Cambridge University Press (1967).
- Chen, J.-Y., (1989). Private communication for methane results. See also Barlow, R. S., Dibble, R. W., Chen, J.-Y. and Lucht, R. P. (1989). Effect of Damhöhler Number on Superequilibrium OH Concentration in Turbulent Nonpremixed Jet Flames. AIAA-89-0061.
- Lewis, G. S., Cantwell, B. J., Vandsburger, U. and Bowman, C. T. (1988). An Investigation of the Structure of a Laminar Non-Premixed Flame in an Unsteady Vortical Flow. *Twenty-Second Symposium (International) on Combustion*, The Combustion Institute, 1988, p. 515.
- Peters, N. and Kee, R. J. (1987). The Computation of Stretched Laminar Methane-Air Diffusion Flames Using a Reduced Four-Step Mechanism. *Comb. Flame* **68** 17.
- Tsuji, H. and Yamaoka, I. (1971). Structure Analysis of Counterflow Diffusion Flames in the Forward Stagnation Region of a Porous Cylinder. *Thirteenth Symposium (International) on Combustion*, The Combustion Institute, 1971, p. 273.

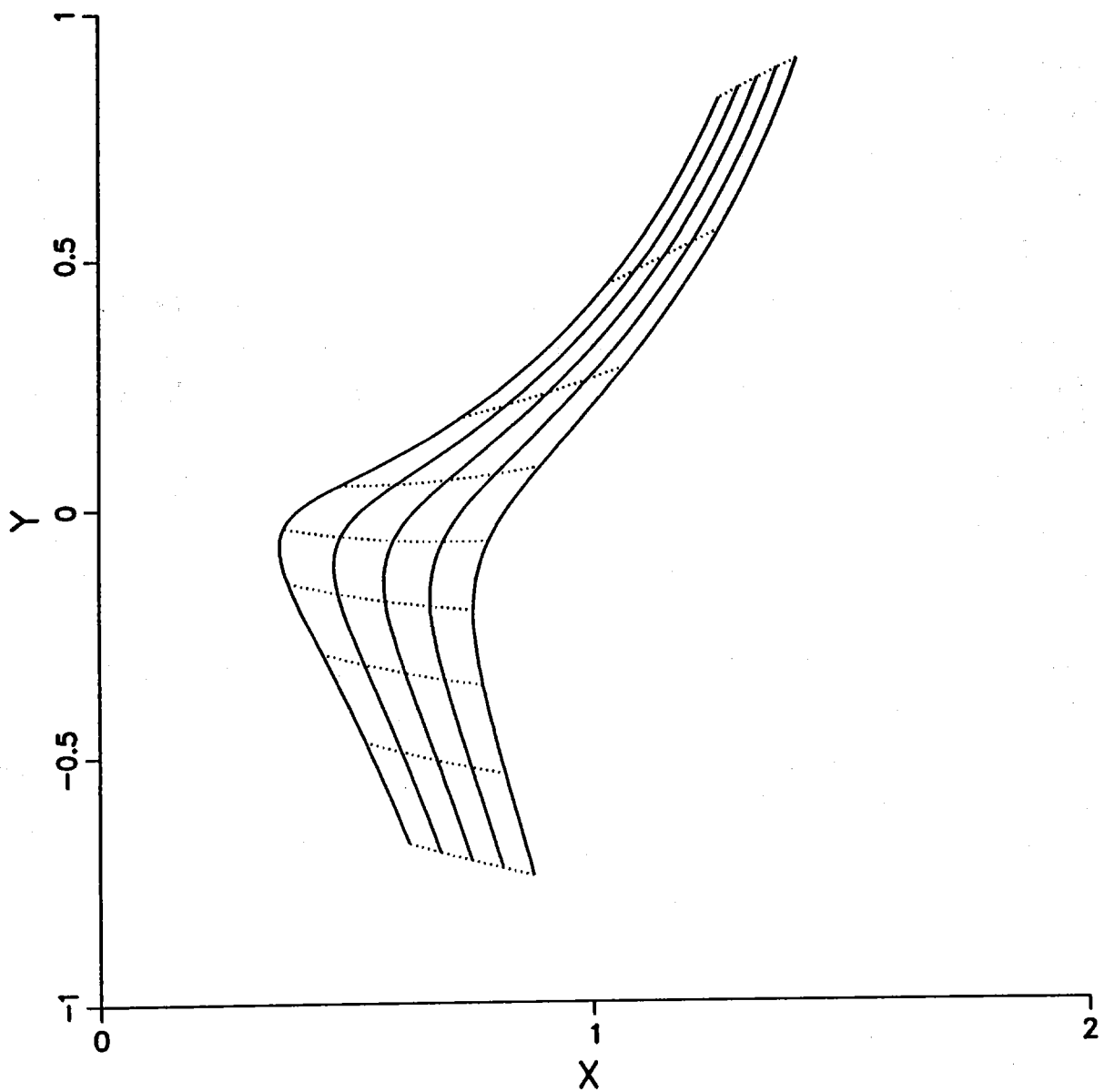


Figure 1. Distortion of scalar isolines in the region between two point vortices. The initially vertical lines were spaced 0.05 units apart in the x direction and show the wrinkle development. The elapsed times, in units of the turn-over time appropriate for each starting radius, are: 0.25, 0.22, 0.20, 0.18 and 0.16; from left-to-right. The vortices are at $(0,1)$ and $(0,-3)$ with clockwise rotation. The dotted lines connect points which started with the same y coordinate.

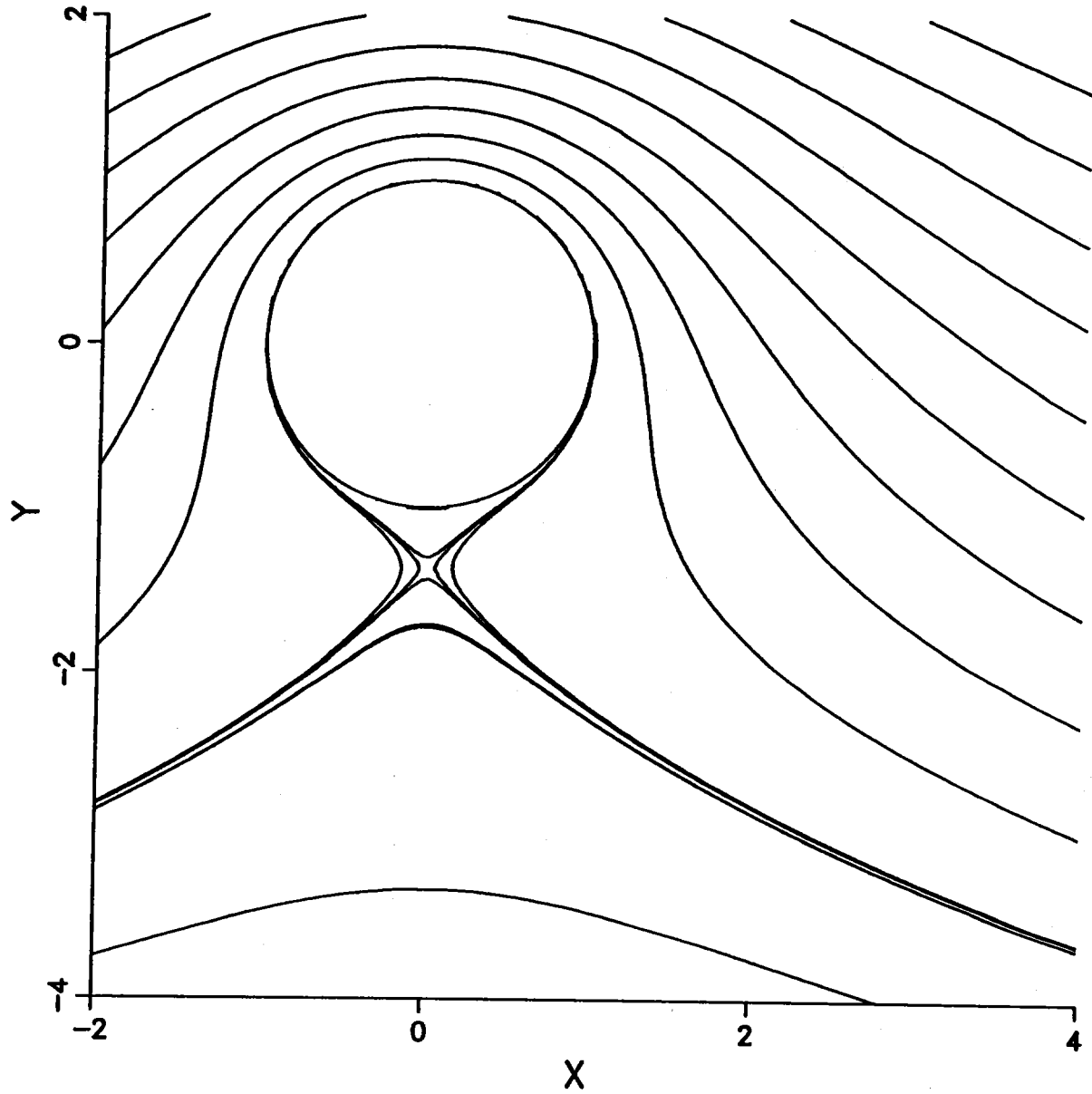


Figure 2. Potential streamlines about a spinning cylinder with the spin large enough to move the stagnation point off the cylinder surface. The circulation in units of $4\pi U_o R_c$, is 1.05. The cylinder rotation is clockwise for left-to-right approach flow, U_o . Equal increments in the stream function are shown with three additional contours drawn to reveal the stagnation-point region.

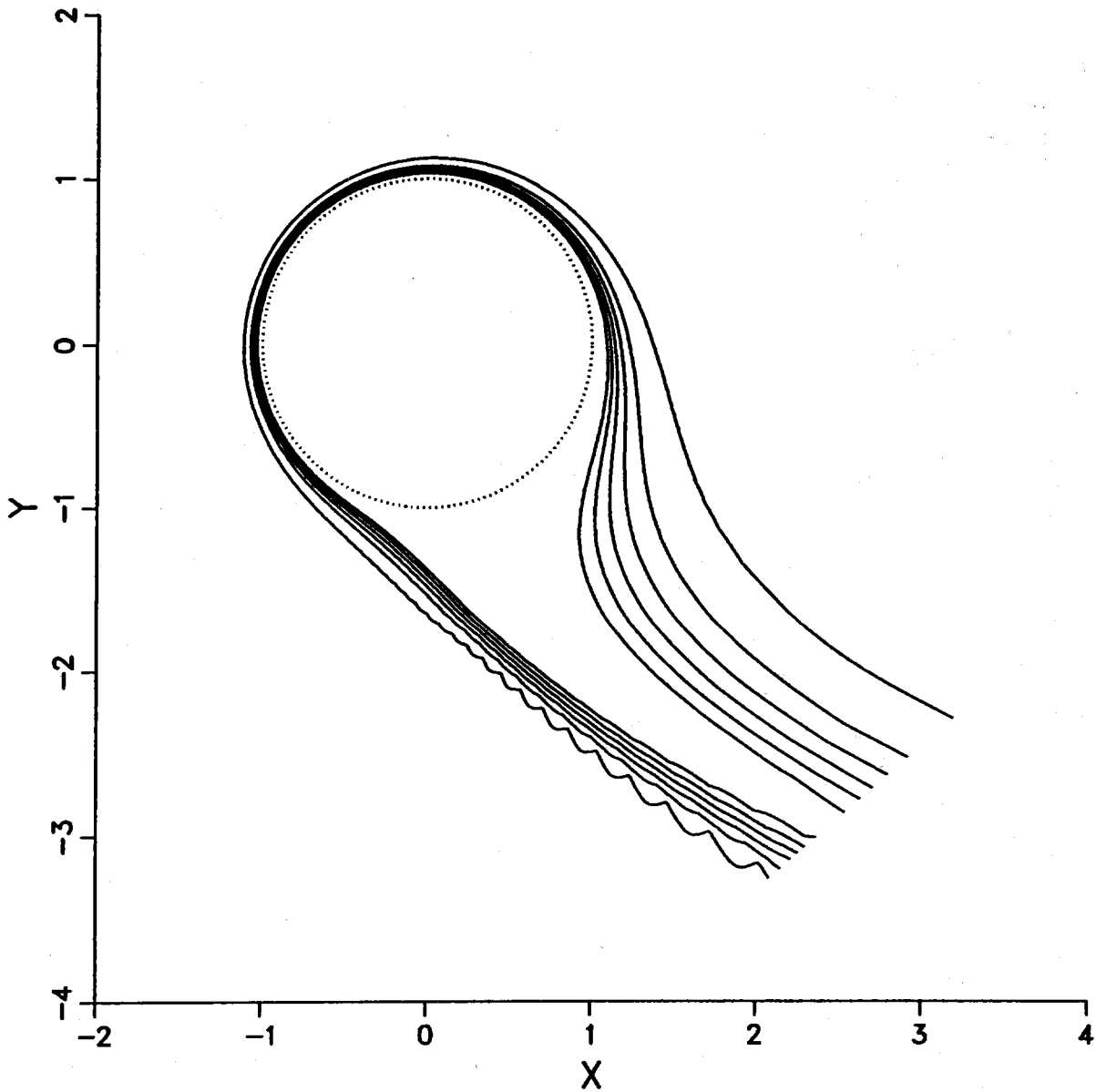


Figure 3a. Mixture fraction iso-lines in potential flow with $\Gamma/(4\pi U_o R_c) = 1.05$ and fuel wall velocity of $0.05 U_o$. At the cylinder, dotted line, the mixture fraction is unity and the drawn iso-lines are $Z = 0.5, 0.4, 0.3, 0.2, 0.1$ and 0.01 . A polar coordinate system has been used between the radii of R_c and $4R_c$ (401 radial grid points with 2.5 degree angular increment); the iso-line wiggles at large radii are artifacts of poor numerical resolution (the grid mesh ratio $R\Delta\theta : \Delta R$ becomes very large and in the wiggle region the convection velocity is diagonal with respect to the local grid axes.)

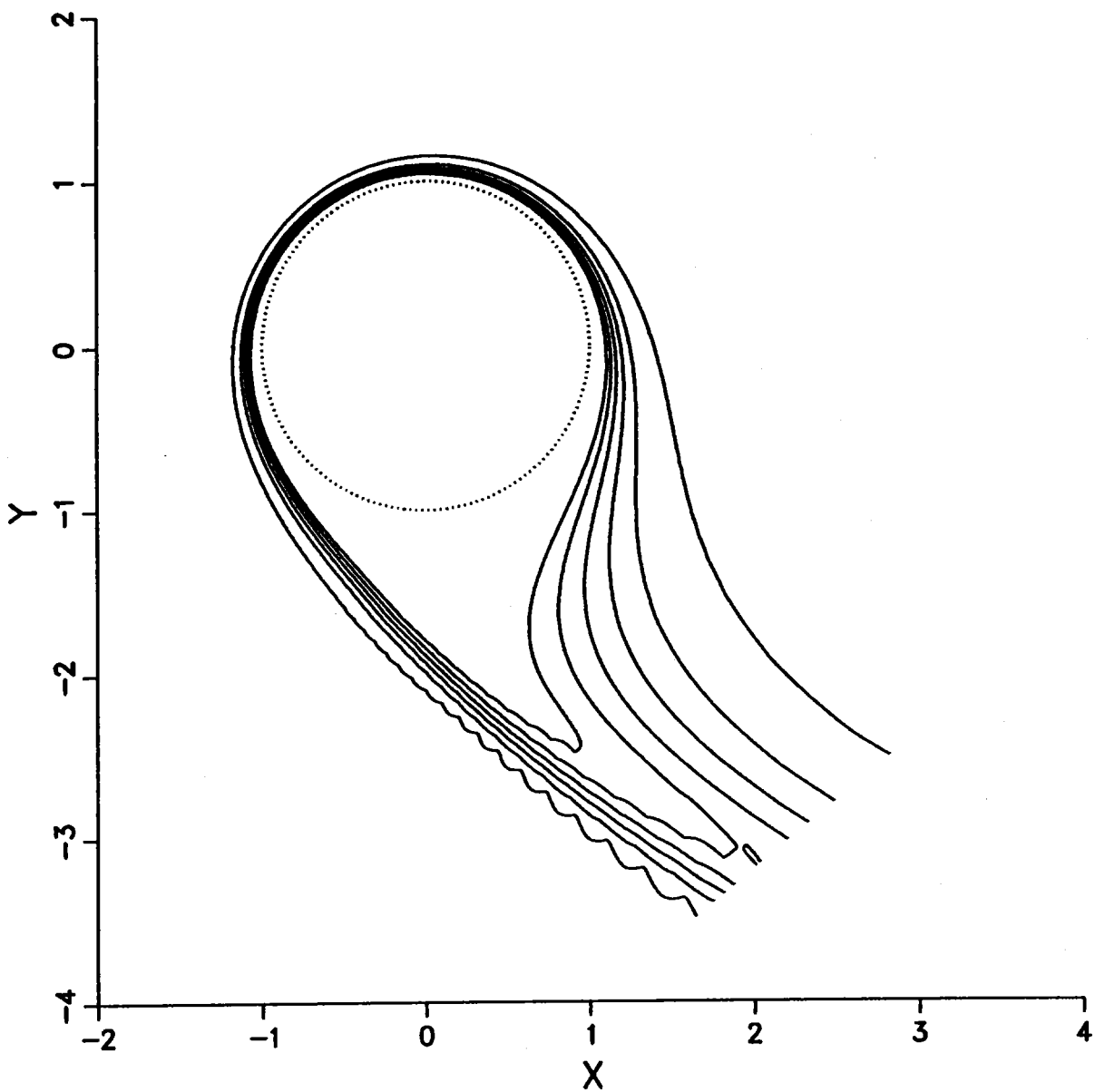


Figure 3b. Mixture fraction iso-lines in potential flow with $\Gamma/(4\pi U_o R_c) = 1.20$ and fuel wall velocity of $0.05 U_o$. Notice that on the back-side of the recirculation region, the scalar gradient is smaller with this faster spin rate. The cylinder rotation is clockwise for left-to-right approach flow, U_o .

UNLIMITED RELEASE

INITIAL DISTRIBUTION

A. H. Laufer
Chemical Sciences Division
Office of Energy Research
Department of Energy
Washington, D.C. 20545

O. Manley
Division of Engineering
and Geosciences
Office of Basic Energy Sciences
Department of Energy
Washington, D.C. 20545

R. S. Marianelli
Chemical Sciences Division
Office of Energy Research
Department of Energy
Washington, D.C. 20545

F. Dee Stevenson
Chemical Sciences Division
Office of Energy Research
Department of Energy
Washington, D.C. 20545

C. Anderson
Dept. of Mathematics
UCLA
405 Hilgard Ave
Los Angeles, CA 90024

H. Aref
AMES Dept. B-010
UCSD
La Jolla, CA 92093-0310

G. Baker
Mathematics Department
Ohio State University
Columbus, OH 43210

J. T. Beale
Mathematics Dept.
Duke University
Durham, NC 27706

R. W. Bilger
Mechanical Engineering
University of Sydney
N.S.W. 2006
AUSTRALIA

K. N. C. Bray
University of Cambridge
Silver St.
Cambridge, CB3 9EW, England

J. E. Broadwell
Graduate Aeronautical Lab, 301-46
California Institute of Technology
Pasadena, CA 91125

F. Browand
Aerospace Engr.
University of Southern California
P. O. Box 77187
Los Angeles, CA 90007

R. Caflisch
Courant Institute of Math
251 Mercer St.
New York, NY 10012

S. M. Candel
Engineering Dept.
Ecole Centrale des Arts
et Manufactures
92295 Chatenay-Malabry
FRANCE

B. J. Cantwell
Aeronautics and Astronautics
Stanford University
Stanford, CA 94305

Jean-Pierre Chollet
Institut de Mecanique
Universite de Grenoble
B. P. 53 X, 38041
Grenoble Cedex
FRANCE

A. Chorin
Mathematics Department
University of California
Berkeley, CA 94720

P. Clavin
Laboratoire de Dynamique
et Thermophysique des Fluides
Universite de Provence
Centre de St-Jerome
13397 Marseille Cedex 13
FRANCE

P. Colella
Mechanical Engineering
University of California
Berkeley, CA 94720

G. M. Corcos
Mechanical Engineering
University of California
Berkeley, CA 94720

W. J. A. Dahm
Dept. of Aerospace Engineering
University of Michigan
Ann Arbor, MI 48109-2140

P. E. Dimotakis
Graduate Aeronautical Lab 301-46
California Inst. of Technology
Pasadena, CA 91125

J. F. Driscoll
Dept. of Aerospace Engineering
University of Michigan
Ann Arbor, MI 48109-2140

F. Durst
Lehrstuhl fur Stromungsmechanik
Universitat Erlangen-Nurnberg
Egerlandstrasse 13
D-8520 Erlangen
WEST GERMANY

H. A. Dwyer
Mechanical Engineering
University of California
Davis, CA 95616

D. Escudie
Ecole Centrale de Lyon
Lab. de Mecanique des Fluides
36, Ave Guy de Collongue
69131 Ecully Cedex
FRANCE

C. Fernandez-Pello
Mechanical Engineering
University of California
Berkeley, CA 94720

C. H. Gibson
AMES Dept. B-010
UCSD
La Jolla, CA 92093-0310

Peyman Givi
Mechanical Engineering
SUNY-Buffalo
Buffalo, NY 14260

P. Haldenwang
Laboratoire de Dynamique
et Thermophysique des Fluides
Universite de Provence
Centre de St-Jerome
13397 Marseille Cedex 13
FRANCE

T. Hasegawa
Mechanical Engineering
Nagoya Institute of Technology
Gokisco-cho, Showa-ku
Nagoya 466,
JAPAN

U. G. Hegde
Aerospace Engineering
Georgia Institute of Technology
Atlanta, GA 30332

J. C. Hill
Chemical Engineering
Iowa State University
Ames, Iowa 50011

J. A. C. Humphrey
Mechanical Engineering
University of California
Berkeley, CA 94720

J. C. Hunt
University of Cambridge
Silver St.
Cambridge, CB3 9EW,
ENGLAND

A. R. Karagozian
5731 Boelter Hall
Mechanical Engineering
UCLA
Los Angeles, CA 90024

L. A. Kennedy
Mechanical Engineering
Ohio State University
Columbus, OH 43210-1107

Robert Krasny
Math Dept.
University of Michigan
Ann Arbor, MI 48109-2140

W. G. Kollmann
Mechanical Engineering
University of California
Davis, CA 95616

M. Koochesfahani
Mechanical Engineering
Michigan State University
East Lansing, MI 48824-1326

J. C. Lasheras
Mechanical Engineering
Univ. of Southern California
Los Angeles, CA 90080-1453

Marcel Lesieur
Institut de Mecanique
Universite de Grenoble
B. P. 53 X, 38041
Grenoble Cedex,
FRANCE

A. Leonard
Graduate Aeronautical Lab 301-4
California Inst. of Technology
Pasadena, CA 91125

P. Libby
AMES Dept. B-010
UCSD
La Jolla, CA 92093-0310

T. Lundgren
Dept. of Aerospace Eng.
University of Minnesota
Minneapolis, MN 55455

P. S. Marcus
Mechanical Engineering
University of California
Berkeley, CA 94720

E. Meiburg
Division of Applied Math
Brown University
Providence RI 02921

D. I. Meiron
Applied Mathematics
217-50 Firestone Lab
California Inst. of Technology
Pasadena, CA 91125

P. Moin
Mechanical Engineering
Stanford University
Stanford, CA 94305

M. G. Mungal
Mechanical Engineering
Stanford University
Stanford, CA 94305

J. Neu
Mathematics Department
University of California
Berkeley, CA 94720

A. K. Oppenheim
Mechanical Engineering
University of California
Berkeley, CA 94720

S. B. Pope
Mechanical Engineering
Cornell University
Ithaca, NY 14853

N. Peters
Institut for Technische Mechanik
RWTH Aachen - Templergraben 64
5100 Aachen, West Germany

J. I. Ramos
Mechanical Engineering
Carnegie-Mellon University
Schenley Park
Pittsburgh, PA 15213-3890

A. Roshko
Graduate Aeronautical Lab, 105-5
California Institute of Technology
Pasadena, CA 91125

R. F. Sawyer
Mechanical Engineering
University of California
Berkeley, CA 94720

K. Seshadri
AMES Dept. B-010
UCSD
La Jolla, CA 92093-0310

J. Sethian
Mathematics Department
University of California
Berkeley, CA 94720

M. Shelly
Dept. of Math, Fine Hall
Princeton University
Princeton, NJ 08544

J. Shepherd
ME, AE & Mechanical
Rensselaer Polytechnic Inst.
Troy, NY 12180-3590

E. D. Siggia
Lab. of Atomic and
Solid State Physics
Cornell University
Ithaca, NY 14853

W. A. Sirignano
Dean, College of Engineering
Univ. of Calif. Irvine
Irvine, CA 92717

P. J. Smith
350 CB, Chemical Engineering
Brigham Young University
Provo, UT 84602

G. Tryggvason
Mechanical Engineering
University of Michigan
Ann Arbor, MI 48109-2125

J. Warnatz
Physikalisch-Chemisches Institut
Universitat Heidelberg
6900 Heidelberg
WEST GERMANY

D. Williams
M. A. E. Dept - E 1
Illinois Institute of Technology
Chicago IL 60616

F. A. Williams
AMES Dept. B-010
UCSD
La Jolla, CA 92093-0310

Gregoire Winckelmans
Calif. Inst. of Technology
205-45
Pasadena, CA 91125

P. R. Woodward
Dept. of Astronomy
University of Minnesota
Minneapolis, MN 55455

N. J. Zabusky
Insitute of Computational Math
Dept. of Mathematics
University of Pittsburgh
Pittsburgh, PA 15260

S. M. Correa
General Electric Corp.
Research and Development
K1-ESB 204
P O Box 8
Schenectady, NY 12301

T. A. Baritaud
Institut Francais du Petrole
BP 311, 92506 Rueil-Malmaison Cedex
FRANCE

H. R. Baum
National Engineering Lab.
National Bureau of Standards
Gaithersburg, MD 20899

L. Campbell
Los Alamos National Laboratory
Los Alamos, NM 87545

R. K. Cheng
Applied Science Division
Lawrence Berkeley Laboratory
Berkeley, CA 94720

J. K. Dukowicz
T-3, MS-B216
Los Alamos National Laboratory
Los Alamos, NM 87545

A. Giovannini
CERT ONERA
BP n 4025
2, Avenue Edouard Belin
31055 Toulouse Cedex
FRANCE

H. Guillard
INRIA
Sophia Antipolis
Route des Lucioles
06560 Valbonne
FRANCE

M. Hyman
T-7, MS-B284
Los Alamos National Laboratory
Los Alamos, NM 87545

R. M. Kerr
Geophysical Turbulence Program
NCAR
Boulder, CO 80307

J. Kim 202A-1
NASA-Ames Research Center
Moffett Field, CA 94035

B. Larrouturou
INRIA
Sophia Antipolis
Route des Lucioles
06560 Valbonne
FRANCE

N. Mansour 202A-1
NASA-Ames Research Center
Moffett Field, CA 94035

P. J. O'Rourke
T-3, MS-B216
Los Alamos National Laboratory
Los Alamos, NM 87545

R. G. Rehm
Mathematical Analysis
Building 101, Room A302
National Bureau of Standards
Gaithersburg, MD 20899

M. M. Rogers 202A-1
NASA-Ames Research Center
Moffett Field, CA 94035

P. Spalart 202A-1
NASA-Ames Research Center
Moffett Field, CA 94035

J. B. Bell, LLNL, L316

L. Cloutman, LLNL, L16

P. M. Gresho, LLNL, L262

W. G. Hoover, LLNL, L794

L. Margolin, LLNL, L16

L. Petzold, LLNL, L316

E. G. Puckett, LLNL, L298

C. K. Westbrook, LLNL, L321

C. E. Leith, LLNL, L16

D. A. Rotman, LLNL, L321

1500	W. Herrmann	8360	W. J. McLean
1510	J. W. Nunziato	Attn:	B. R. Sanders, 8360A
1413	G. G. Weigand	8361	W. T. Ashurst
1512	J. C. Cummings	8361	D. R. Hardesty
1513	D. W. Larson	8361	A. R. Kerstein
6000	D. L. Hartley	8361	R. E. Mitchell
Attn:	A. W. Snyder, 6400	8362	P. K. Barr
6420	J. V. Walker	8362	K. D. Marx
Attn:	M. Berman, 6427	8362	D. L. Siebers
8000	J. C. Crawford	8364	D. D. Dandy
Attn:	E. E. Ives, 8100	8364	S. B. Margolis
	R. J. Detry, 8200	8364	S. C. Johnston
	R. C. Wayne, 8400	8535	Publications Div. / Technical Library Processes Division, 3141
	P. E. Brewer, 8500	3141	Technical Library Processes Division, (3)
8240	C. W. Robinson	8524	Central Technical Files (3)
Attn:	J. H. Chen, 8244		
	R. Chenoweth, 8244		
	C. M. Hartwig, 8244		
8245	R. J. Kee		
Attn:	A. E. Lutz, 8245		
8300	P. L. Mattern		
Attn:	R. W. Rohde, 8310		
	W. Bauer, 8340		
8350	J. S. Binkley		
Attn:	R. J. Carling, 8357		
8351	R. S. Barlow		
8351	J. Y. Chen		
8351	R. W. Dibble		
8351	R. P. Lucht		
8351	R. W. Schefer		
8353	G. A. Fisk		
Attn:	J. A. Miller, 8353		



8232-2/069750



00000002 -



8232-2/069750



00000002 -



8232-2/069750



00000002 -

